PLEASE DO NOT REMOVE THIS PAGE

cogent
engineering

PRODUCTION & MANUFACTURING | RESEARCH ARTICLE

Model-driven design of a fast material removal electrical discharge machine

Bo Hu[1], John P.T. Mo[1]*, Songlin Ding[1] and Milan Brandt[1]

*Corresponding author: John P.T. Mo, School of Aerospace, Mechanical and Manufacturing Engineering, RMIT University, Melbourne, Victoria, Australia
E-mail: john.mo@rmit.edu.au

Abstract: In order to minimize cost of machining, modern aerospace components are highly unitized to utilize functions of multi-axes CNC machining centres. However, PCD tools are preferred for machining of titanium alloys and metal matrix composites but they are hard to grind. A new fast material removal electric discharge machine suitable for small PCD workpiece machining has been developed from an innovative model consisting both high and low frequency response actuators and a dual stage non-linear control algorithm. This innovative approach has been proved successful in the single axis machine prototype and the fast material removal rate has been verified a series of tests and the outcomes were verified.

Subjects: Industrial Engineering & Manufacturing; Manufacturing Engineering; Systems & Control Engineering

Keywords: polycrystalline diamond tools; PCD machining; electric discharge grinding; dual stage non-linear control; erosion modelling; innovative design and manufacturing

1. Introduction

The excellent mechanical properties of exotic materials such as titanium alloys and metal matrix composites (MMCs) have led to many applications in aerospace and high value added industries. Due to the need for structural integrity and cost minimisation, the aerospace industry is designing highly unitised components that combine a large number of features on one product. These features can

ABOUT THE AUTHORS

The machine tools research group led by Professor John P.T. Mo with leading research members Professor Milan Brandt and Associate Professor Songlin Ding has been working on a number of industry sponsored research projects including development of new machining theories for exotic materials and continuous chatter prevention. This new research in polycrystalline diamond tools grinding is highly successful to assist a Melbourne based CNC machine manufacturer to develop a new product that has been sort after in the tooling industry. Several students have completed their PhD studies in this topic. The latest PhD graduate, Bo Hu has pioneered the concept of dual machine axes that can adapt to the much faster erosion response required for electric spark erosion. The outcome is a much faster material erosion process. This successful research lays the foundation for further research investigation into a full scale machine tool for polycrystalline diamond material machining.

PUBLIC INTEREST STATEMENT

In order to minimize cost of machining, modern aerospace components are designed to make use of complicated functions of multi-axes CNC machining centres. However, the machining time for one component can be exceptionally long posting significant risk of tool wear and breakage. Polycrystalline diamond (PCD) tools are therefore preferred to be used, especially for machining exotic materials such as titanium alloys and metal matrix composites. Since PCD is the hardest tool material, sharpening PCD tools is difficult with traditional grinding technology. This paper describes the design of a fast PCD tool grinding machine by a model-driven approach. This innovative machine design includes a dual stage axis and algorithm for controlling electric pulse to maximize erosion. The approach has been proved successful in the single axis machine prototype and the fast material removal rate has been verified.

cogent ··oa

be machined by multi-axes CNC machine tools using a large variety of tools. For example, small diameter carbide tools are used in the milling of intricate titanium components to achieve accurate dimensions when drilling multi-layer hybrid stacks (Ramulu, Branson, & Kim, 2001). However, these cutters must operate at a low cutting speed due to their short tool life at higher cutting speed runs (Pan, Ding, & Mo, 2014). Even at lower speeds, in certain applications, some tools only last for a few minutes. Low tool life presents significant challenges to manufacturers. With the increased utilization of titanium alloys and MMC in aerospace, medical and other industries, there is a pressing need for design of new machining systems to improve productivity.

Recently, advanced materials such as cubic boron nitride (CBN) (Dogra, Sharma, Sachdeva, Suri, & Dureja, 2010), polycrystalline cubic boron nitride (PCBN), binderless cubic boron nitride (BCBN), and polycrystalline diamond (PCD) (Arsecularatne, Zhang, & Montross, 2006) have become available for cutting tools. Among these new materials, CBN and PCBN tools are not suitable for machining titanium alloys because of their poor performance (Rahman, Wang, & Wong, 2006). The high reactivity of titanium alloys causes excessive wear of CBN/PCBN tools. In contrast the extreme hardness and excellent thermal conductivity of PCD makes it the most promising cutting tool material for titanium machining (Wang, Wong, & Rahman, 2005) and drilling of composite/titanium stacks (Park, Beal, Kim, Kwon, & Lantrip, 2011).

Due to their hardness, it is extremely difficult to grind PCD to a shape suitable for cutting purposes, particularly when the work holding space is limited on small complex parts. Currently, PCD tools are only made as large inserts of simple geometry on large diameter cutters. No small diameter milling tool can be found on the market and hence machining of complex titanium parts relies on less effective carbide tools. Due to difficulties in fabricating complex PCD cutters, and the lack of a suitable grinding process to manufacture accurate geometries on small diameter tools, there has been little research about the fundamental requirements of manufacturing systems in complex features milling of titanium.

Electrical discharge machining (EDM) is a manufacturing process that has the capability of removing exotic materials such as PCD by applying electric sparks to the materials (Yan, Huang, Chow, & Tsai, 1999). This process has the advantage that it is basically usable for any material that conducts electricity, irrespective of its hardness (Singh, Maheshwari, & Pandey, 2004). However, for small workpiece such as a PCD tool, the traditional tool making EDM configuration is not suitable for small movement grinding requirements (Davydov, Volgin, & Lyubimov, 2004; Yan, Fang, & Liu, 2012). This paper outlines a modeling approach to design a fast EDM with advanced mechanisms and control systems. The effectiveness of this EDM is verified on a prototype.

2. Literature review

In EDM process, exotic materials are eroded from a conductive workpiece by applying a high frequency electrical pulse to it via a vibrating electrode or a moving wire. A servo system control the movement of the electrode to approach the workpiece but to keep a small gap, across which an insulating dielectric fluid flows (Zhou & Han, 2009). A high temperature plasma channel is generated when the high voltage is applied on the gap to break down the dielectric and it evaporates the workpiece before it. After the plasma channel occurs, the electrical power source is off for a similar period allowing the dielectric fluid to flush the debris away from the gap. The gap width, which is in the range of 10–100 μm, is critical for the EDM material removal rate and surface finish because poor gap width control can cause high probability of abnormal discharges, for example short circuit, open circuit and arc. In the mean time, the short pulse period of 0.1–40 μs and the random scattering movement of debris particles need a fast response servo system of EDM to quickly adjust the gap width for debris expulsion and short dielectric breakdown (Jiang, Zhao, Xi, & Gu, 2012). However, there are limits for the response of traditional servo systems, which use a DC servomotor to covert the rotary motion to linear motion by a ball screw arrangement. A limit of those servo systems is its accuracy due to backlash, irregular friction, and the resolution of an encoder for the position measurement.

Many attempts have been made to improve the EDM gap width control for high removal rate. Adaptive control algorithms were applied to EDM servo systems for the optimal gap width adjustment based on identification of its discharge states (Wang & Rajurkar, 1992). Robust control, sliding mode control (Chang, 2002) and fuzzy control (Çaydaş, Hasçalık, & Ekici, 2009; Zhang et al., 2002) were used to enhance the robustness to variation of EDM machining conditions and minimize the abnormal discharge states due to the stochastic characteristics of EDM process. However, the traditional EDM servo actuators were slow in response and inaccurate in position resolution.

To tackle these problems, piezoelectric actuator was introduced for fast adjustment of the gap width of EDM. Its high bandwidth can achieve 1 kHz, higher than those of the conventional DC or linear motor. Kunieda, Takaya, and Nakano (2004) installed a piezoelectric actuator under a workpiece to control the gap width of dry EDM and its simulation results showed that the piezoelectric actuator improved the material removal rate. These fast response actuators with resolution in the nanometer range, were used in micro-EDM machining to fabricate microstructures on workpieces. For example, micro holes with diameters less than 45 μm were drilled (Liu, Lauwers, & Reynaerts, 2009). Similarly, 200 × 200 μm grooves could be cut on PCD with good surface roughness of 0.10 μm (Yan, Watanabe, & Aoyama, 2014).

Assisted by the piezoelectric actuator or an ultrasonic wave generator, many researchers improved the EDM removal rate by ultrasonic vibration, which could also lower heating damage by a better flushing (Singh, Singh, & Singh, 2013; Wei, Zhao, Hu, & Ni, 2012). To synchronize of piezoelectric movement and EDM pulses, Tong, Li, Wang, and Yu (2008) proposed a macro/micro-dual-feed structure that consists of a linear motor as the macro-drive and a piezoelectric actuator as microfeeding mechanism to keep the desirable discharge gap. The good surface finish with a Ra value of 0.37 μm was reported and the high machining repeatability error of <0.7%. How to cooperate the dual actuators for the good performance and the robust stability is critical. Ding, Tomizuka, and Numasato (2000) used two steps: the first step was to design the macro-drive system for basic performance and the second step is to design the micro-drive system by loop shaping for superior performance of the overall system. Schroeck, Messner, and McNab (2001) reduced the dual stage system into a single loop system by adding an auxiliary compensator.

To design a new EDM system with non-traditional axes control and different response characteristics, a proven methodology should be adopted due to its complexity and accuracy requirements. Garcia, Keshmiri, and Stastny (2015) found that nonlinear model predictive control was not robust enough when there were errors and uncertainties in the physical system. They proposed a new systematic approach using frequency-dependent weighting matrices and verified its effectiveness in an unmanned aerial system. Tang, Huang, and Deng (2012) used Takagi-Sugeno fuzzy model and generalized predictive control tp protect their vehicle from spinning thereby improving its performance around corners. In this case, some training data had been used to tune the model. In their research to minimize modelling complexity, Kondratenko, Klymenko and Al Zu'bi (2013) developed a general method to reduce the number of fuzzy rules in the controller, without affecting its performance. It is therefore important that this research adopts a model based design approach to minimize any unexpected motion and performance.

3. Design objectives of the EDM

Literature review shows that a more comprehensive model driven design process is required to achieve a fast EDM. The design objectives of the new electrical discharge machine include:

3.1. Reducing the EDM machine cost

A ultra-fast servo response servo system is developed in the new EDM machine and so the EDM machine has capabilities to prevent a workpiece from damaging the rotating electrode wheel under the environment disturbance. This can reduce the base cost of EDM and an economic spindle, which drive the electrode wheel, can be chosen to further decrease the machine price. The cost of the new machine may be just one-tenth of commercial EDM machines, whose prices are around $400,000.

3.2. Increasing the EDM removal rate

The new fast response servo system has two stage actuators for each axis: a piezoelectric actuator which has fast response (1 kHz) but short stroke (100 μm) for quickly adjustment of the gap between the workpiece and electrode wheel to achieve the high ratio of normal discharges; a linear motor which has long stroke (1 m) but slow response (1–20 Hz) to cover a big dimension workpiece. The new EDM machine has faster cutting rate by minimizing abnormal discharges of EDM, for instance short circuit and open circuit.

3.3. Improving the surface finish of workpieces

With the dual stage actuators design, the new EDM machine is able to have multi-rate control scheme to reduce the amount of arcs that two consecutive discharges occur at a same location during EDM process. The discharge voltage and current of the new EDM machine is processed with a rate of 250 M/s by a FPGA chip, which is fast enough to discriminate EDM discharge status in a real time with the amount of 1 M/s pulse rate. The sampling rate of the piezoelectric control loop can be set as 40 kHz for the new EDM machine. As a result, its control period is around 25 μs and the servo system can adjust the gap for each discharge, which has 10 μs on-time and 10 μs off-time. By quickly increase the gap width, the probability of arc is able to extinct. Therefore, the roughness of workpieces can be reduced.

4. Control scheme for EDM

Figure 1 illustrates the control block diagram of this EDM servo system.

It is understood from literature that the electrode wear is slow. The EDM servo system should change the gap width by controlling the PCD workpiece position. The model of the linear actuator can be expressed as:

$$M_1(x_1, t)\ddot{x}_1(t) + C_1(x_1, \dot{x}_1, t)\dot{x}_1(t) + q_1(x_1, t) = u_1(t) \tag{1}$$

where $M_1(x_1) \in R^{3 \times 3}$ is the inertia matrix, $C_1(x_1, \dot{x}_1, t)\dot{x}_1(t) \in R^3$ is the vector relating centrifugal and Coriolis force, $g(x_1) \in R^3$ is the gravitational vector, and $x_1, u \in R^3$ are the displacement and driving force vector. During the eroding period, the linear actuator is required to track the slow and time-varying material removal rate of EDM by maintaining the gap width between 10 and 50 μm. The error can be expressed

$$e_1(t) = Y(t) - X(t) \to 0 \quad as \quad t \to \infty \tag{2}$$

Figure 1. Control block diagram of the dual stage servo system.
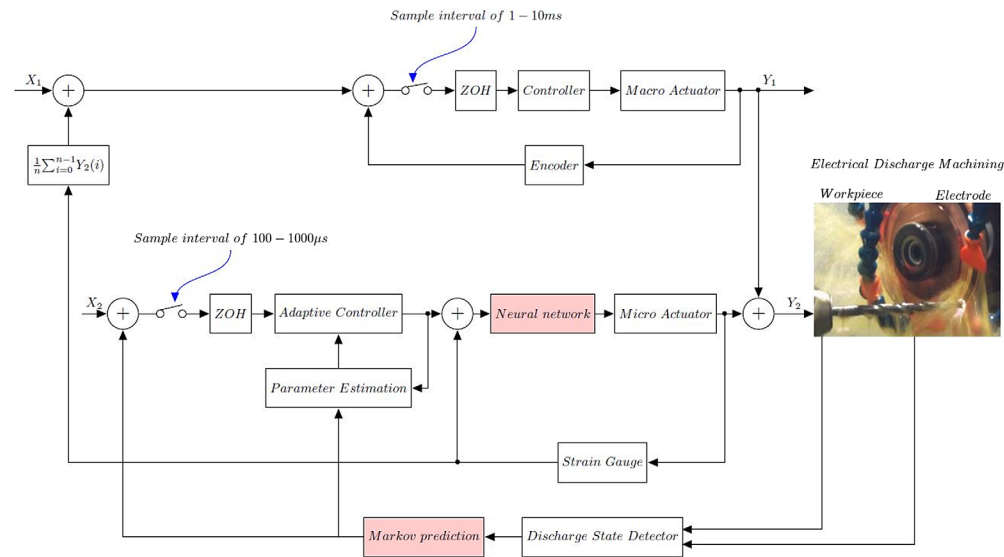
The controller is

$$f(t) = k_p e_1(t) + k_i \int_0^\infty e_1(t) dt \qquad (3)$$

The transfer function of the linear actuator is

$$\frac{Y_1(s)}{X_1(s)} = \frac{C_1(s)G_1(s)}{1 + C_1(s)G_1(s)} \qquad (4)$$

where

$$C_1(s) = K_p + \frac{K_i}{s} \qquad (5)$$

$$G_1(s) = \frac{k_s}{s^2 + 2\xi\omega_n s + \omega_n^2} \qquad$$

The discharge state variation at high frequency is adjusted by the piezoelectric actuator by compensating the high frequency error signal of the gap voltage, which are processed by a high pass filter. The transfer function of this high pass filter is:

$$H(s) = \frac{s}{s + 1} \qquad (6)$$

The position reference of the piezoelectric actuator is:

$$x_2 = H(s)e_1 \qquad (7)$$

Considering that the PCD workpiece with a mass of M is on the top of the piezoelectric actuator (PZT), the following equation can describe the motion of the PZT:

$$M_2 \ddot{x}_2(t) + C_2 \dot{x}_2(t) = u_2(t) \qquad (8)$$

where C_2, $x_2(t)$, $u_2(t)$ are the dielectric damping coefficient, the PZT displacement, and the force from the expansion of PZT element. The transfer function of the PZT control loop is:

$$\frac{Y_2(s)}{X_2(s)} = \frac{C_2(s)G_2(s)}{1 + C_2(s)G_2(s)} \qquad (9)$$

where

$$C_2(s) = K_{p2} + \frac{K_{i2}}{s} \qquad (10)$$

$$G_1(s) = \frac{k_s}{s^2 + \xi_2 s} \qquad$$

The PCD workpiece position Y is:

$$Y = y_1 + y_2 \qquad (11)$$

Due to the nonlinearity of EDM erosion, the advanced control scheme has advantages to improve its erosion efficiency. A two-layer feed forward neural network was introduced for high removal rate, shown in Figure 2.

Figure 2. The neural network control algorithm for EDM gap width.
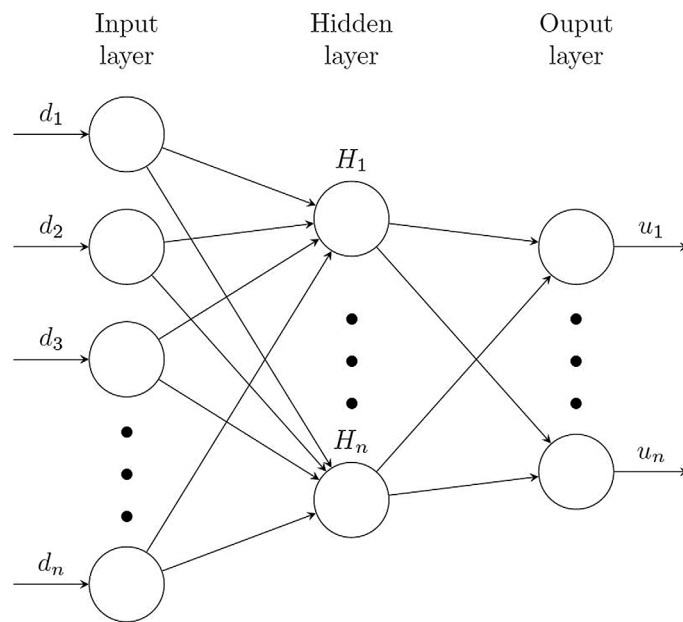
It is used to compensate the position error of the micro actuator, including an input buffer, a non-linear hidden layer and a linear output layer. Each neuron as a node in Figure 2 has an output given by

$$y_i = f\left(\sum_{j=1}^{r} w_{ij}x_j + b_i\right) \tag{12}$$

where w_{ij} is the weight, x_j is the ith input, b_i is a bias, and $f(x)$ is an activation function. The activation function must be continuous and differentiable over all time. In this study, the activation function in the hidden layer is nonlinear as a tan-sigmoid function and that in the output layer is linear. Therefore, the feed-forward outputs of the hidden layer and the output layer are shown in (9),

$$y_{1i} = f_1\left(\sum_{j=1}^{r} w_{1ij}x_j + b_{1i}\right), \quad i = 1, 2, \ldots, r \tag{13}$$

$$y_{2k} = f_2\left(\sum_{j=1}^{m} w_{2ki}y_{1i} + b_{2k}\right), \quad k = 1, 2, \ldots, m$$

The method to find the right weights is a back-propagation method. The weight updating law is to minimize the objective function E, which is given by

$$E = \frac{1}{2}\sum_{k}\left(d_k - y_k\right)^2 \tag{14}$$

Using the gradient descent method, the weight updating formulas of the output layer and the hidden layer are:

$$\Delta w_{2ki} = -\eta\frac{\partial E}{\partial w_{2ki}} = -\eta\frac{\partial E}{\partial y_{2k}}\frac{\partial y_{2k}}{\partial w_{2ki}} = \eta\delta_{ki}y_{1i} \tag{15}$$

$$\Delta b_{2ki} = -\eta\frac{\partial E}{\partial b_{2ki}} = -\eta\frac{\partial E}{\partial y_{2k}}\frac{\partial y_{2k}}{\partial b_{2ki}} = \eta\delta_{ki}$$

and

$$\Delta w_{1ij} = -\eta \frac{\partial E}{\partial w_{1ij}} = -\eta \frac{\partial E}{\partial y_{2k}} \frac{\partial y_{2k}}{\partial y_{1i}} \frac{\partial y_{1i}}{\partial w_{1ij}} = \eta \delta_{ki} p_j \tag{16}$$

$$\Delta b_{1ij} = -\eta \frac{\partial E}{\partial b_{1ij}} = \eta \delta_{ij}$$

where

$$\delta_{ki} = (t_k - y_{2k})$$

$$\delta_{ij} = e_i f_1^1$$

$$e_i = \sum_{k=1}^{m} \delta_{ki} w_{ki} \tag{17}$$

Considering that EDM discharges do not take place uniformly in time due to the random distribution of eroded particles, Wang and Rajurkar (1992) introduced EDM discharge states into the control loop as stochastic disturbance to reduce the variance caused by process noise. However, they used the time ratios of discharge states as the feedback signal, which is detected from those previous discharges. In this project, we proposed a new method to predicate the incoming discharge states based on the previous discharges and Markov model. It is supposed provide more accurate feedback signal. The matrix of EDM discharge state transition probabilities in Figure 3 can be expressed

$$P = \begin{bmatrix} P_{ss} & P_{sa} & P_{sp} & P_{so} \\ P_{as} & P_{aa} & P_{ap} & P_{ao} \\ P_{ps} & P_{pa} & P_{pp} & P_{po} \\ P_{os} & P_{oa} & P_{op} & P_{oo} \end{bmatrix}_{4 \times 4} \tag{18}$$

Figure 3. EDM discharge status prediction model.
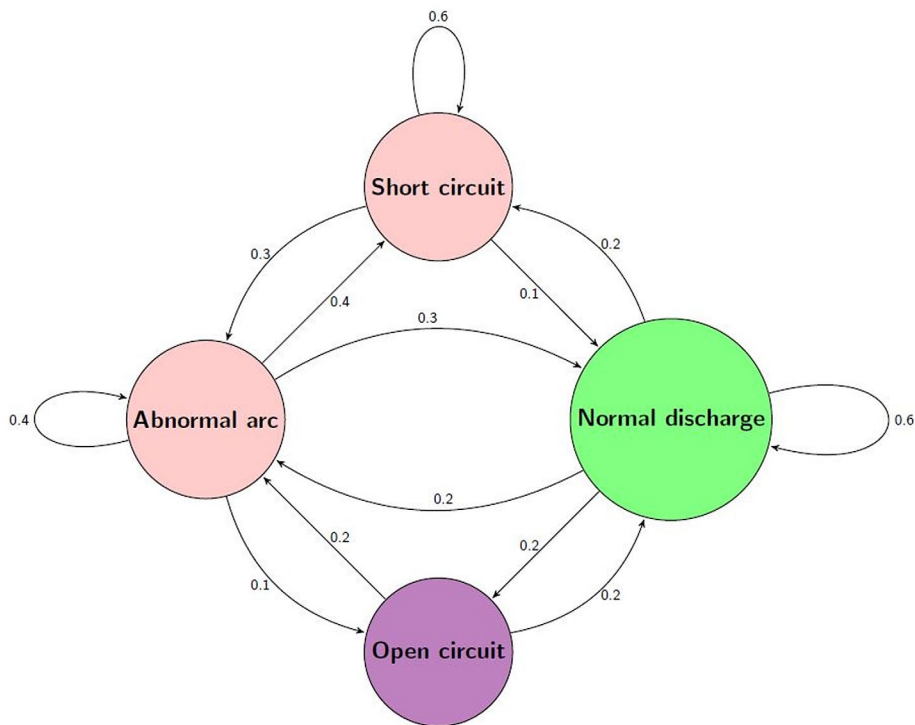
where p_{ij} is the probabilities from i discharge state to j state and s, a, p, o are four type of discharge states: short circuit, arc, normal discharge and open circuit.

In order to simplify the calculation, there is the Markov assumption that the probability of an observation at time t_n only depend on the observation at time t_{n-1}. $w_i(n)$ (n = 0, 1, 2,...) is the probability of an EDM discharge state at time t_n, the Markov assumption can be expressed as:

$$p\left(w_{n-1}, w_{n-2}, \ldots, w_1\right) \approx p\left(w_n | w_{n-1}\right) \text{ for a sequence } \{w_1, w_2, \ldots, w_n\} \tag{19}$$

The vector of the probability of EDM discharges is

$$W(n) = \left[w_s(n), w_a(n), w_p(n), w_o(n)\right]^T \tag{20}$$

where

$$0 \leq w_s(n), w_a(n), w_p(n), w_o(n) \leq 1 \tag{21}$$

$$w_s(n) + w_a(n) + w_p(n) + w_o(n) = 1$$

The matrix in Equation (16) can be expressed as $P = (p_{ij})_{4 \times 4}$ and the coming EDM discharge state can be predicted by

$$W_i(n+1) = p_{is}w_s(n) + p_{ia}w_a(n) + p_{ip}w_p(n) + p_{io}w_o(n) \text{ for } i = s, a, p, o \tag{22}$$

This formula can be expressed in matrix format:

$$W(n+1) = PX(n) \tag{23}$$

$$P \geq 0, \quad \sum_{i=1}^{4} p_{ij} = 1$$

So the EDM discharge state at time from now can be obtained by recursive formula:

$$W(n) = P^n W(0) \tag{24}$$

where $W(0) = [w_s(0), w_a(0), w_p(0), w_o(0)]'$ is the current EDM discharge state vector.

Figure 4. Structure of the new EDM machine.

cogent ··engineering
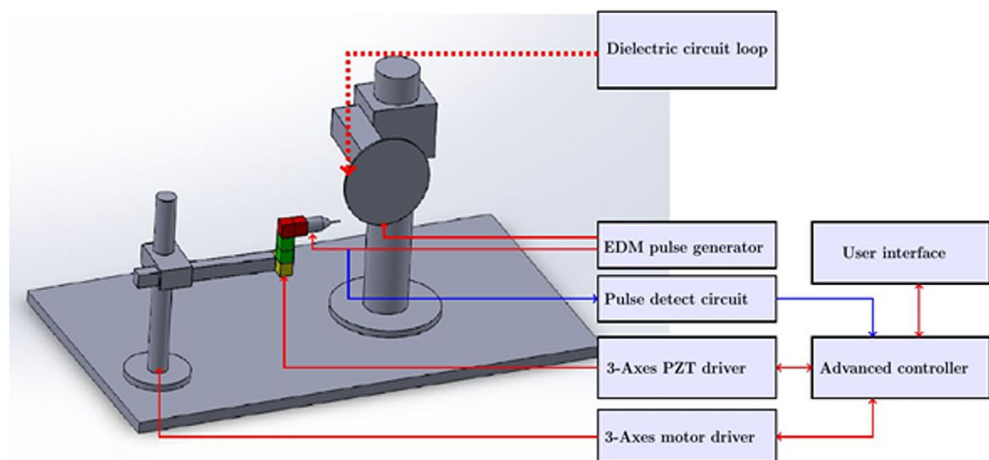
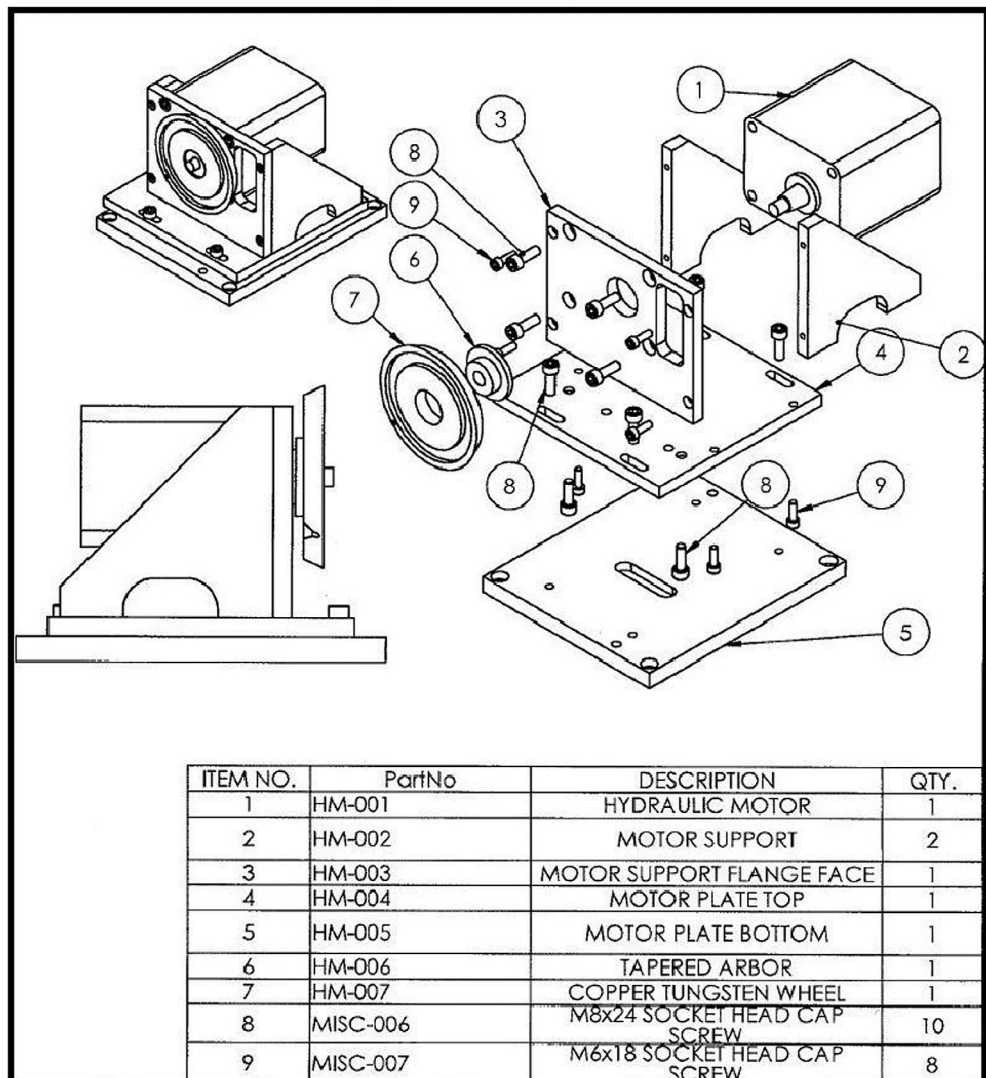**Table 1. Feature designed into the new EDM basic structure**

Feature	Description of feature
First stage actuator	A linear motor and its controller. The stroke is 25 mm
Second stage actuator	A piezoelectric actuator and its controller. The stroke is 100 μm and the position resolution is 5 nm
Pulse discrimination system	A discharge voltage adapter, a pulse current adapter, and a 250 M/s A/D card
Advanced controller	A National Instrument PXI controller with a real time system and all of advanced control algorithms are running in this hardware
Electrode wheel	A copper tungsten wheel is driven at a fixed rotating speed of 250 RPM by a hydraulic motor
Pulse generator	A commercial pulse generator which can provide the pulse with various on/off time and polarity to the workpiece and the electrode wheel
Dielectric circulation system	The dielectric can be pumped into the tank to submerge the workpiece and the electrode wheel. After process, the liquid is drained to the accumulation tank, sitting under the working tank, through a filter

5. Structure of the new EDM

Figure 4 illustrated the basic structure of the new EDM machine for fast erosion of PCD material in applications such as shaping of cutting tools.

The main design features are summarized in Table 1.

Figure 5. Detailed design of new EDM.

ITEM NO.	PartNo	DESCRIPTION	QTY.
1	HM-001	HYDRAULIC MOTOR	1
2	HM-002	MOTOR SUPPORT	2
3	HM-003	MOTOR SUPPORT FLANGE FACE	1
4	HM-004	MOTOR PLATE TOP	1
5	HM-005	MOTOR PLATE BOTTOM	1
6	HM-006	TAPERED ARBOR	1
7	HM-007	COPPER TUNGSTEN WHEEL	1
8	MISC-006	M8x24 SOCKET HEAD CAP SCREW	10
9	MISC-007	M6x18 SOCKET HEAD CAP SCREW	8

Table 2. Capabilities in the new EDM	
Capabilities	**Description of capabilities**
Cutting the thin layer of PCD and tungsten carbide tools, whose depth resolution is 3 μm	This is due to two new technologies: the piezoelectric actuator, which can precisely control the position of its end-effector with the resolution of 5 nm; and a new control scheme that the new machine controls the distance between the workpiece and the rotating electrode wheel instead of the feed rate control of commercial EDM machine
Cutting the big PCD and tungsten carbide tools, whose lengths are around 20 mm	The normal servo axis is able to travel at least 20 mm to move the workpiece
Roughing and finishing operation of EDM process	Various EDM parameters can be set, including on-time, off-time, polarity, open circuit voltage, electrical current, etc
Observing and recording the plasma channel ignition, evaporation, expansion, and collapse	The EDM process proceeds in a transparent environment and the dielectric fluid is in the laminar flow, therefore, an external optical emission spectroscopy can detect the plasma composition, density, and temperature. It helps the full understanding of EDM eroding mechanism and gives the direction of EDM erosion advancement
Observing the debris expulsion trajectory with high speed camera	The machine chamber is installed with Perspex materials to allow the electric discharge points to be visible from outside so that the high speed camera can take a video record
Easily apply advanced control algorithm to the new EDM machine	The control algorithms developed in Matlab can be embedded into the real time control loop of the EDM machine due to LabView software compatibility
Pulse discrimination functions	The EDM machine has Tektronix P5200A voltage converter, which has a bandwidth of 50 MHz, to convert a high discharge voltage of 300 V and 120 to 5 V. A hall effect current probe is also included to convert the EDM discharge electrical current to a low voltage of 5 V. A National Instruments 5,761 sampling card can do the analog to digital conversion with 250 M/s with a FPGA chip. A VHDL program is under development to discriminate the EDM discharge status
Showing the EDM discharge waveform in a real time way	The expensive oscilloscope can be saved for operators to tune the EDM machine for the optimal performance

The detailed design of the new EDM is shown in Figure 5. The machine is mounted with copper tungsten electrode wheel driven by hydraulic motor and has a range of new capabilities in comparison to traditional EDM machines as shown in Table 2.

Using the model, to reduce the prototype development cost, a single axis EDM machine was developed to verify the effects of the new technologies, as shown in Figure 6. The control algorithm as explained in the previous section is implemented in a software of EDM erosion control is shown in Figure 7.

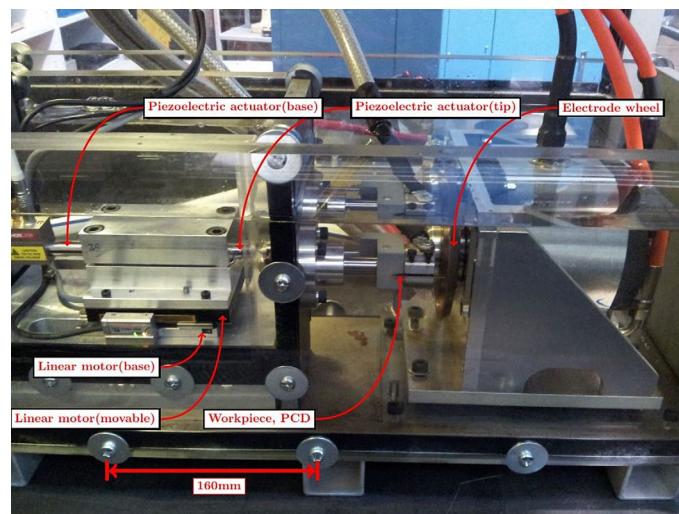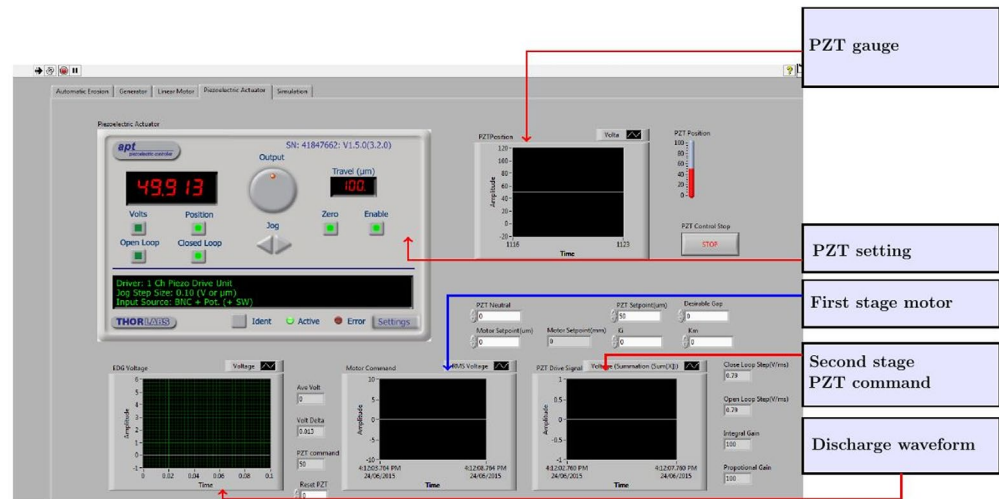**Figure 6. A single axis EDM with dual stage actuators.**

Figure 7. Software developed in Labview.

7. Results and discussion

The experimental results were obtained by operating the new EDM machine to erode a CMX850 PCD and tungsten carbide workpiece. As illustrated in Figure 8, the new EDM machine is cutting a PCD piece. The lighting point is the spark from a plasma during discharge process. The operating parameters of this machine was on-time: 20 μs, off-time: 20 μs, ignition voltage: 120 V, current: 12 A.

The experiments show that the software can drive the dual stage actuators to cut the workpiece more than 3 mm. Figure 9 shows how the PCD workpiece surface finish was measured under the microscope after EDM erosion.

Figure 10 shows the PCD and tungsten carbide surface after EDM roughing operation. The upper area is the tungsten carbide surface and the lower part of the photo belongs to PCD. The top surface is the original surface finish as a reference. The low surface is under a cut by EDM and its cutting length is around 3 mm as previously noted.

Figure 8. The new EDM machine in operation.
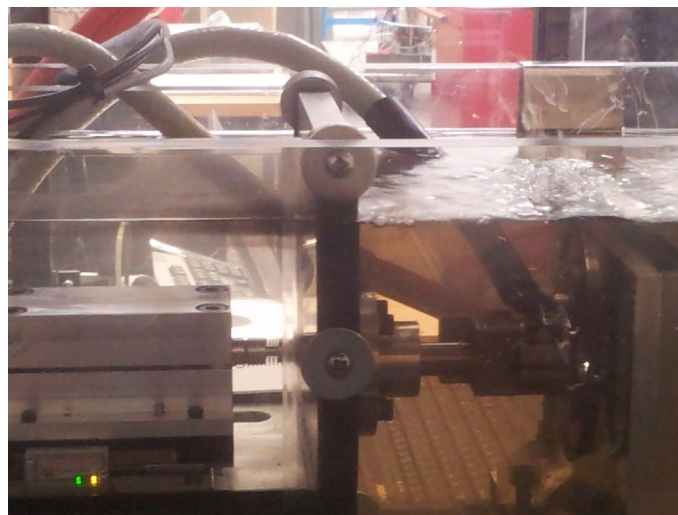
Figure 9. The PCD workpiece under the microscope after erosion on EDM.
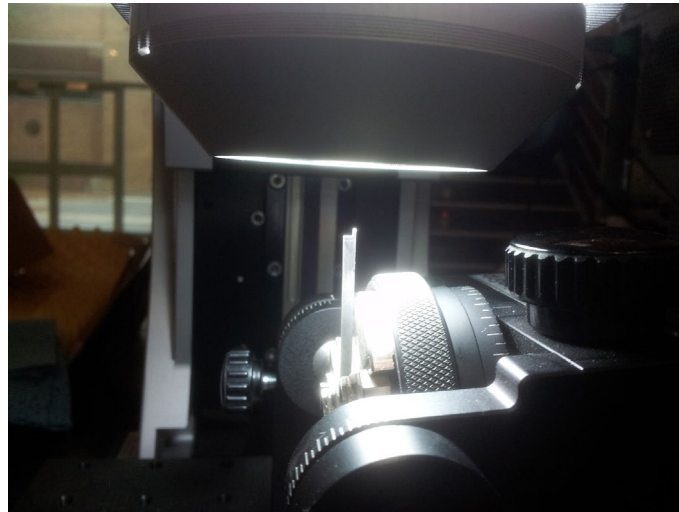
The PCD roughness after EDM roughing operation has been measured by a 3D optical microscope. The surface variation of PCD surface (i.e. the measurement of R_a) as shown in Figure 11 was measured on a straight line highlighted by a red mark line in Figure 10.

Using a number line of measurements, the 3D surface after EDM roughing operation can be reconstructed as shown in Figure 12.

The cutting length of 3 mm is much longer than the stroke of the PZT (100 µm). The surface finish over this length was maintained consistently. It shows that the dual stage servo system of the EDM has a capability to fabricate big workpieces with fine surface finish created by the PZT precise performance. In this experiment, the removal rate was 0.44 mm³/min which was similar to using larger more powerful EDM (Hua et al., 2015) and at the same time maintaining the PCD surface finish R_a value at 0.24 µm for the entire length.

With the high speed camera, the debris expulsion trajectories are recorded, illustrated in Figure 13. The high speed camera recorded an individual discharge process, which has the on time of 100 µs and the off time of 10,000 µs. The eight photos with a continuous sequence showed that the molten debris splashed in all directions and can exist long time (around 80 µs) than the normal on time of a

Figure 10. PCD and tungsten carbide surface under microscope.
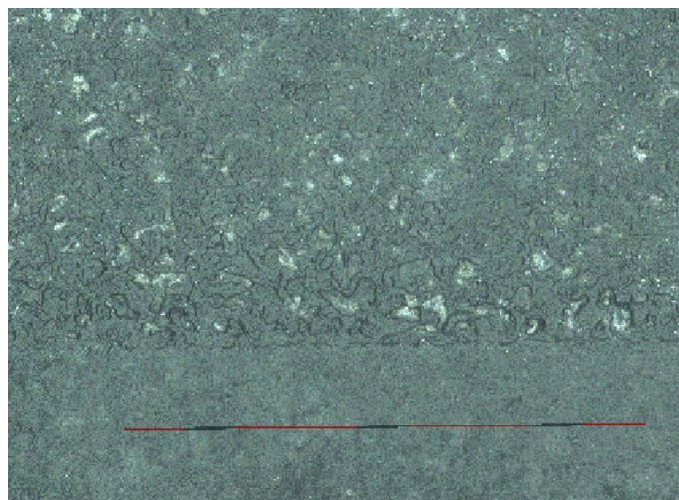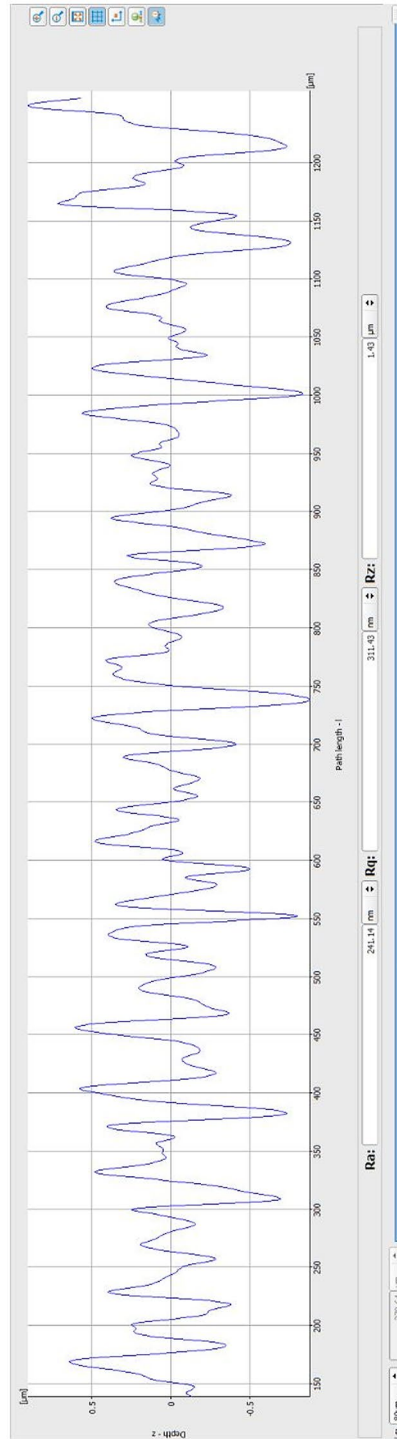
Figure 11. Surface variation measured by Alicona microscope.

**Figure 12. A 3D elaboration of the PCD roughness.**
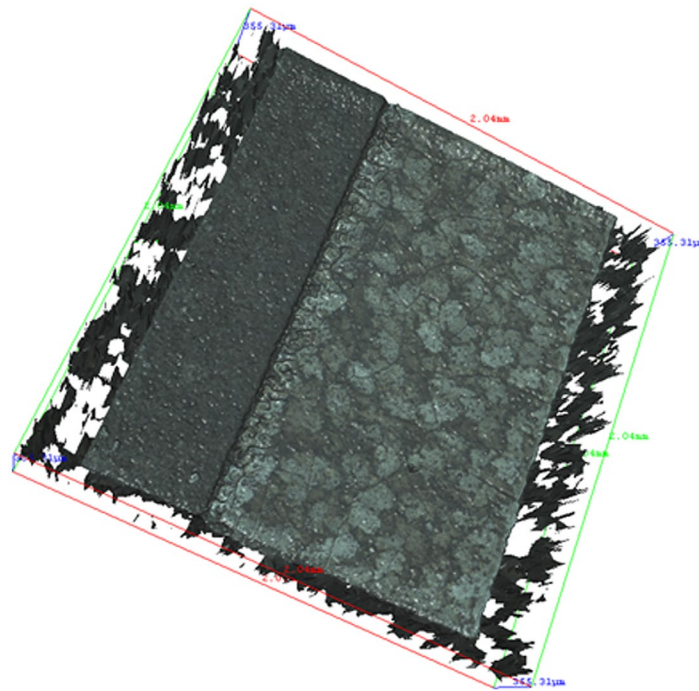
Figure 13. The sequence of individual discharge process by a high speed camera.
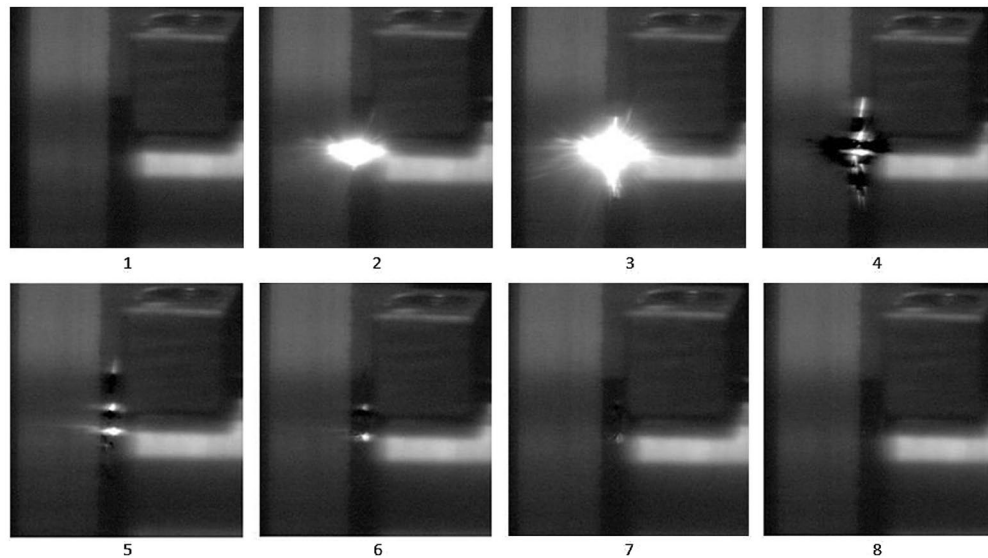
discharge (10–20 μs). Since the off times of EDG processes are often set as around 20 μs for the high material removal rate, the debris particles from the earlier discharges can lead to that new discharges take place around them. Bringing the low conductivity between the gap, the long-time molten debris can have great impact on those crater morphology and their distribution.

The PZT has very high position resolution of 5 μm and therefore the gap width can be precisely measured for the workpiece to touch the wheel before experiment and retract a distance for EDM erosion. The relation between its discharge status and gap widths are obtained as shown in Figure 14. The nonlinearity gives a good model for EDM gap control for high ratio of normal discharge, which can enhance the removal rate and surface finish.

cogent ·· engineering

Figure 14. Relation between EDM discharge states and gap width.
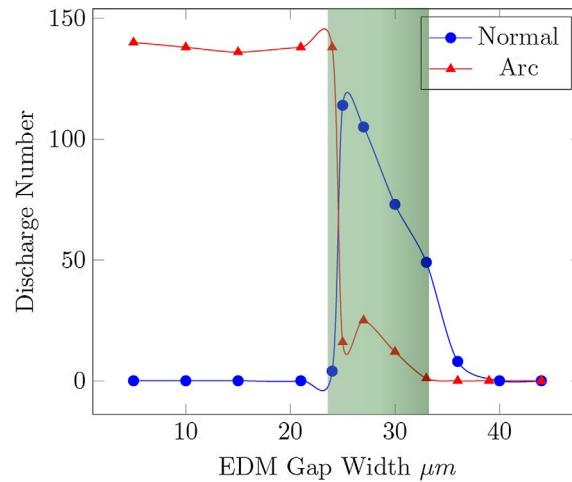
8. Conclusion

A new fast material removal electric discharge machine suitable for small PCD workpiece machining has been developed. In order to achieve the desirable machining capabilities, the design of the new EDM has been driven by an EDM stochastic erosion model. This model shows the relationship between the gap width and the discharge status, and illustrates the need for fast response to keep the electric discharge gap within very tight tolerance. The model has been made with the assumption of a fast positional response from the machine and hence a dual stage servo system has been included in the design with a PZT. Due to the relative limited distance control of the PZT, a normal linear servomotor is also incorporated into the design to fabricate the required size of the workpieces.

The software control system of the new EDM is developed from a multi-rate control scheme in which each stage control loop has various sampling rate and a low pass filter is used to transfer data between two stage actuators. The model predicts the probability of EDM discharge status in the next pulsing cycle based on Markov model and has proved to work well in the prototype.

The success of this new EDM has been proven by a series of tests on a single axis machine prototype that has been built for this research. The prototype has shown superior performance over some of our previously reported research, being able to sustain good surface finish over a long distance on the workpiece. Further work is continuing to improve the control algorithm and system structure making it ready for multiple axes investigation.

Author details
Bo Hu[1]
E-mail: s3406249@student.rmit.edu.au
John P.T. Mo[1]
E-mail: john.mo@rmit.edu.au
ORCID ID: http://orcid.org/0000-0002-0697-7504
Songlin Ding[1]
E-mail: songlin.ding@rmit.edu.au
Milan Brandt[1]
E-mail: milan.brandt@rmit.edu.au
[1] School of Aerospace, Mechanical and Manufacturing Engineering, RMIT University, Melbourne, Victoria, Australia.

References
Arsecularatne, J. A., Zhang, L. C., & Montross, C. (2006). Wear and tool life of tungsten carbide, PCBN and PCD cutting tools. *International Journal of Machine Tools & Manufacture, 46*, 482–491. http://dx.doi.org/10.1016/j.ijmachtools.2005.07.015
Çaydaş, U., Hasçalık, A., & Ekici, S. (2009). An adaptive neuro-fuzzy inference system (ANFIS) model for wire-EDM. *Expert Systems with Applications, 36*, 6135–6139.
Chang, Y. -F. (2002). VSS controller design for gap control of EDM. *JSME International Journal Series C, 45*, 712–721. http://dx.doi.org/10.1299/jsmec.45.712
Davydov, A. D., Volgin, V. M., & Lyubimov, V. V. (2004). Electrochemical machining of metals: Fundamentals of electrochemical shaping. *Russian Journal of Electrochemistry, 40*, 1230–1265. http://dx.doi.org/10.1007/s11175-005-0045-8
Ding, J., Tomizuka, M., & Numasato, H. (2000). *Design and robustness analysis of dual stage servo system* (pp. 2605–2609). In American Control Conference, Chicago, IL.

Dogra, M., Sharma, V. S., Sachdeva, A., Suri, N. M., & Dureja, J. S. (2010). Tool wear, chip formation and workpiece surface issues in CBN hard turning: A review. *International Journal of Precision Engineering and Manufacturing, 11*, 341–358. http://dx.doi.org/10.1007/s12541-010-0040-1

Garcia, G., Keshmiri, S., & Stastny, T. (2015). Nonlinear model predictive controller robustness extension for unmanned aircraft. *International Journal of Intelligent Unmanned Systems, 3*, 93–121. http://dx.doi.org/10.1108/IJIUS-01-2015-0002

Hu, B., Lim, C. Ding, S., L. Rahim, M. Z., Brandt, M., & Mo, J. P. T. (2015). Experimental study of wheel rotating speed effect on electrical discharge grinding. *Applied Mechanics and Materials, 697*, 275–279. doi:10.4028/www.scientific.net/AMM.697.275

Jiang, Y., Zhao, W., Xi, X., & Gu, L. (2012). Adaptive control for small-hole EDM process with wavelet transform detecting method. *Journal of Mechanical Science and Technology, 26*, 1885–1890. http://dx.doi.org/10.1007/s12206-012-0410-y

Kondratenko, Y. P., Klymenko, L. P., & Al Zu'bi, E. Y. M. (2013). Structural optimization of fuzzy systems' rules base and aggregation models. *Kybernetes, 42*, 831–843. http://dx.doi.org/10.1108/K-03-2013-0053

Kunieda, M., Takaya, T., & Nakano, S. (2004). Improvement of dry EDM characteristics using piezoelectric actuator. *CIRP Annals - Manufacturing Technology, 53*, 183–186. http://dx.doi.org/10.1016/S0007-8506(07)60674-X

Liu, K., Lauwers, B., & Reynaerts, D. (2009). Process capabilities of micro-EDM and its applications. *International Journal of Advanced Manufacturing Technology, 47*, 11–19.

Pan, W., Ding, S., & Mo, J. P. T. (2014). Thermal characteristics in milling Ti6Al4V with polycrystalline diamond tools. *The International Journal of Advanced Manufacturing Technology, 75*, 1077–1087. http://dx.doi.org/10.1007/s00170-014-6094-y

Park, K.-H., Beal, A., Kim, D., Kwon, P., & Lantrip, J. (2011). Tool wear in drilling of composite/titanium stacks using carbide and polycrystalline diamond tools. *Wear, 271*, 2826–2835. http://dx.doi.org/10.1016/j.wear.2011.05.038

Rahman, M., Wang, Z.-G., & Wong, Y.-S. (2006). A review on high-speed machining of titanium alloys. *JSME International Journal, Series C, 49*, 11–20. http://dx.doi.org/10.1299/jsmec.49.11

Ramulu, M., Branson, T., & Kim, D. (2001). A study on the drilling of composite and titanium stacks. *Composite Structures, 54*, 67–77. http://dx.doi.org/10.1016/S0263-8223(01)00071-X

Schroeck, S. J., Messner, W. C., & McNab, R. J. (2001). On compensator design for linear time invariant dual input single output systems. *IEEE/ASME Transactions on Mechatronics, 6*, 50–57. http://dx.doi.org/10.1109/3516.914391

Singh, J., Singh, S., & Singh, G. (2013). Study of surface roughness for discontinuous ultrasonic vibration assisted electric discharge machining using RSM. *International Journal of Engineering Research and Technology, 2*, 727–737.

Singh, S., Maheshwari, S., & Pandey, P. C. (2004). Some investigations into the electric discharge machining of hardened tool steel using different electrode materials. *Journal of Materials Processing Technology, 149*, 272–277. http://dx.doi.org/10.1016/j.jmatprotec.2003.11.046

Tang, G. Y., Huang, D. M., & Deng, Z. (2012). T-S fuzzy model based generalized predictive control of vehicle yaw stability. *Kybernetes, 41*, 1261–1268.

Tong, H., Li, Y., Wang, Y., & Yu, D. (2008). Servo scanning 3D micro-EDM based on macro/micro-dual-feed spindle. *International Journal of Machine Tools and Manufacture, 48*, 858–869. http://dx.doi.org/10.1016/j.ijmachtools.2007.11.008

Wang, W. M., & Rajurkar, K. P. (1992). Modeling and adaptive control of EDM systems. *Journal of Manufacturing Systems, 11*, 334–345. http://dx.doi.org/10.1016/0278-6125(92)90062-K

Wang, Z. G., Wong, Y. S., & Rahman, M. (2005). High-speed milling of titanium alloys using binderless CBN tools. *International Journal of Machine Tools & Manufacture, 45*, 105–114. http://dx.doi.org/10.1016/j.ijmachtools.2004.06.021

Wei, C., Zhao, L., Hu, D., & Ni, J. (2012). Electrical discharge machining of ceramic matrix composites with ceramic fiber reinforcements. *The International Journal of Advanced Manufacturing Technology, 64*, 187–194.

Yan, B. H., Huang, F. Y., Chow, H. M., & Tsai, J. Y. (1999). Micro-hole machining of carbide by electric discharge machining. *Journal of Materials Processing Technology, 87*, 139–145. http://dx.doi.org/10.1016/S0924-0136(98)00345-8

Yan, J., Watanabe, K., & Aoyama, T. (2014). Micro-electrical discharge machining of polycrystalline diamond using rotary cupronickel electrode. *CIRP Annals - Manufacturing Technology, 63*, 209–212.

Yan, M.-T., Fang, G.-R., & Liu, Y.-T. (2012). An experimental study on micro wire-EDM of polycrystalline diamond using a novel pulse generator. *International Journal of Advanced Manufacturing Technology, 66*, 1633–1640.

Zhang, J. H., Zhang, H., Su, D. S., Qin, Y., Huo, M. Y., Zhang, Q. H., & Wang, L. (2002). Adaptive fuzzy control system of a servomechanism for electro-discharge machining combined with ultrasonic vibration. *Journal of Materials Processing Technology, 129*, 45–49. http://dx.doi.org/10.1016/S0924-0136(02)00573-3

Zhou, M., & Han, F. (2009). Adaptive control for EDM process with a self-tuning regulator. *International Journal of Machine Tools and Manufacture, 49*, 462–469. http://dx.doi.org/10.1016/j.ijmachtools.2009.01.004

cogent • engineering